

## $^{25}\text{Mg}(d, ^3\text{He})^{24}\text{Na}$ reaction at 29 MeV and a spectroscopic analysis of the levels of $^{24}\text{Na}$

J. Verotte, G. Berrier-Ronsin, S. Fortier, E. Hourani, J. Kalifa, J. M. Maison, L-H. Rosier, and G. Rotbard  
*Institut de Physique Nucléaire, Institut National de Physique Nucléaire et de Physique des Particules—Centre National  
 de la Recherche Scientifique, 91406 Orsay Cedex, France*

B. H. Wildenthal

*The University of Texas at Dallas, Box 830688, Richardson, Texas 75083-0688*

(Received 14 October 1997)

The  $^{25}\text{Mg}(d, ^3\text{He})^{24}\text{Na}$  reaction has been investigated at 29 MeV incident energy. Spectra were measured at  $\theta_{\text{lab}} = 10^\circ$  and  $18^\circ$ . Observations using a split-pole magnetic spectrograph have been made of 56 levels of  $^{24}\text{Na}$  in the range of excitation energy between 0 and 7.3 MeV. Most of these have been identified with  $^{24}\text{Na}$  levels which have been previously observed by other techniques. From the ratios of the experimental as well as distorted-wave Born approximation (DWBA)-predicted cross sections at the two angles, the population through the pickup of an  $l_p = 1$  proton has been established (or confirmed) for the twelve levels at  $E_x = 3.372, 3.745, 3.936, 4.524, 5.192, 5.250, 5.452, 5.846, 5.863, 6.905, 7.084,$  and  $7.246$  MeV. Spectroscopic factors were obtained from the comparison of the experimentally measured cross sections at the two angles with the DWBA-predicted cross sections. The experimental values of spectroscopic factors and excitation energies for positive-parity states were compared with the results of a recent, complete  $sd$ -shell space, shell-model calculation. In conjunction with the results of various previous works, this comparison leads to the identification of 19 shell-model levels with experimental levels, and thus allows the removal of ambiguities existing in the current literature for the  $J^\pi$  values of some  $^{24}\text{Na}$  states with  $E_x < 3.7$  MeV.  
 [S0556-2813(98)00703-1]

PACS number(s): 21.10.Jx, 21.10.Hw, 25.45.Hi, 27.30.+t

### I. INTRODUCTION

The  $(d, ^3\text{He})$  reaction has been widely studied on  $sd$ -shell target nuclei. Much spectroscopic information about the states populated in this one-proton pickup reaction, such as excitation energies, orbital angular momenta of the transferred proton, and spectroscopic factors, is presented in Refs. [1,2]. However, most of these previous studies have been done with an energy resolution ( $\Delta E \approx 80\text{--}100$  keV) which, in many cases, did not allow the unambiguous identification of the observed peaks with excitation energies known accurately from other experiments. This is especially true for some peaks which result from the pickup of a proton from the subshells  $1p_{1/2}$  and  $1p_{3/2}$  and which lie at excitation energies of several MeV.

Therefore, the first motivation of a new study of the  $(d, ^3\text{He})$  reaction on some  $sd$ -shell target nuclei which was recently undertaken in this laboratory was to accurately determine excitation energies by taking advantage of the improved experimental energy resolution which results from using a tandem accelerator in conjunction with a split-pole magnetic spectrograph. Thus far, the  $^{27}\text{Al}(d, ^3\text{He})^{26}\text{Mg}$  and  $^{29}\text{Si}(d, ^3\text{He})^{28}\text{Al}$  reactions have been investigated at  $E_d = 29$  MeV. The experimental spectra were obtained with an overall energy resolution of 16 and 22 keV for the levels of  $^{26}\text{Mg}$  and  $^{28}\text{Al}$ , respectively, and the excitation energies were obtained with an accuracy of 5 keV for sixty-five  $^{26}\text{Mg}$  levels [3] and fifty-five  $^{28}\text{Al}$  levels [4] ranging in excitation energy up to 9.7 and 6.7 MeV, respectively. Among these levels, eight  $^{26}\text{Mg}$  levels and four  $^{28}\text{Al}$  levels were attributed to the pickup of the proton from the  $1p$  shell.

The current availability of shell-model calculations done

for  $sd$ -shell nuclei with an Hamiltonian which is valid for the whole  $sd$  shell (the USD Hamiltonian [5]) was a second motivation for a new study of this reaction. These calculations yield predictions for many spectroscopic features of the positive-parity states and the comparison of these predictions with experimental results for as many nuclear levels as possible is a necessary step to extend the validation of the calculations. Shell-model predictions for excitation energies and spectroscopic factors of states resulting from the pickup of one proton in the  $2s$  and  $1d$  orbits were thus compared with the experimental values obtained in the above quoted studies of the  $(d, ^3\text{He})$  reaction at  $E_d = 29$  MeV and the identification with shell-model predicted levels could be made for twenty-four  $^{26}\text{Mg}$  levels and twenty-one  $^{28}\text{Al}$  levels in Refs. [3] and [4], respectively. The agreement between the experimentally measured and shell-model predicted spectroscopic factors and excitation energies was so good for most of the identified pairs of levels that it was suggested to use this identification in some cases as a spectroscopic tool to determine unknown  $J^\pi$  values of experimental levels.

This paper presents the results of a new study of the  $^{25}\text{Mg}(d, ^3\text{He})^{24}\text{Na}$  reaction also done at  $E_d = 29$  MeV. In a previous study of this reaction at  $E_d = 52$  MeV [6], eighteen peaks were observed and values of the spectroscopic factors obtained for sixteen of them from the distorted-wave Born approximation (DWBA) analysis of the experimental angular distributions. However, the energy resolution ( $\Delta E \sim 80$  keV) of this previous experiment was a limitation for the study of the odd-odd  $^{24}\text{Na}$  final nucleus at excitation energies higher than a few MeV, so that nine levels with  $E_x > 3.6$  MeV (five of them being populated through  $l_p = 1$  transitions) could not be identified with levels of the current literature [1]. As for

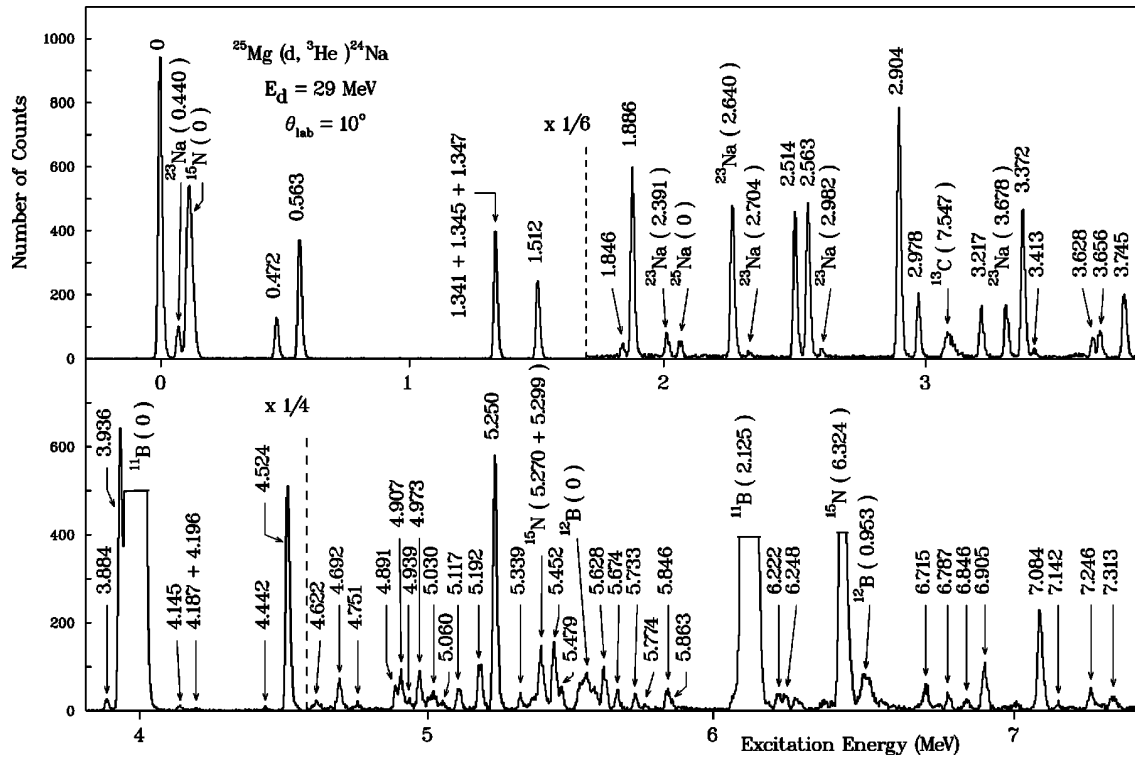


FIG. 1. Spectrum of the  $^{25}\text{Mg}(d, ^3\text{He})^{24}\text{Na}$  reaction taken at  $\theta_{\text{lab}}=10^\circ$  for an accumulated charge of 2000  $\mu\text{C}$ . The excitation energies are from Ref. [2] unless more accurate values are available from this work (see Sec. III and Table I). The peaks which are due to the  $(d, ^3\text{He})$  reaction on nuclei other than  $^{25}\text{Mg}$  are identified with the excitation energies in the corresponding final nuclei.

the other recent studies noted above [3,4], the first goal of this new study was to determine the excitation energies accurately enough to make this identification possible. Furthermore, the  $^{24}\text{Na}$  nucleus seems a convenient case to check the use of the identification of a pair of experimentally measured and shell-model predicted levels as a spectroscopic tool for the  $J^\pi$  assignments, since there are ambiguities in Ref. [2] for the  $J^\pi$  values of some low-energy levels [for instance, the levels at  $E_x=1.345$ , 1.512, 2.563, 2.978, 3.217, and 3.656 MeV with  $J^\pi=3^+(+)$ ,  $5^+(3^+)$ ,  $4^+(2^+)$ ,  $2^+(3^+)$ ,  $4^+(2^+)$ , and  $2^+(1^+)$ , respectively]. The removal of these ambiguities through a careful comparison of the shell-model predictions with the experimental information which is available from the present work and from various other sources was the second goal of this work.

## II. EXPERIMENTAL PROCEDURE AND ANALYSIS OF SPECTRA

A 29 MeV deuteron beam from the upgraded Orsay MP Tandem Van de Graaff accelerator was focused onto a target placed at the center of a scattering chamber, with the beam then being stopped in a graphite Faraday cup connected to a current integrator. The magnesium target was prepared by *in vacuo* evaporation of metallic magnesium (enriched to 96% in  $^{25}\text{Mg}$ ) onto a carbon backing ( $\sim 5 \mu\text{g cm}^{-2}$  thick). This target had been previously used for studying the elastic scattering of 25 MeV  $^3\text{He}$  [7] and the number of  $^{25}\text{Mg}$  nuclei was thus determined to be equal to  $N(^{25}\text{Mg})=(13.51 \pm 0.68) \times 10^{17}$  nuclei  $\text{cm}^{-2}$ .

The  $^3\text{He}$  particles were momentum analyzed with an Enge split-pole magnetic spectrograph. The detection system

has been described previously [8]. The spectrograph horizontal entrance aperture was set to  $\pm 1.5^\circ$ , which leads to a solid angle  $\Omega \approx 1.6$  msr.  $^3\text{He}$  spectra were measured at  $\theta_{\text{lab}}=10^\circ$  and  $18^\circ$ . The complete spectrum at each angle was measured using a single value of the magnetic field of the spectrograph. The charge  $Q$  accumulated for each spectrum was equal to 2000  $\mu\text{C}$ . The  $^3\text{He}$  spectrum taken at  $\theta_{\text{lab}}=10^\circ$  is displayed in Fig. 1. The full width at half maximum is about 18 keV. In addition to the peaks which are due to the population of levels in  $^{24}\text{Na}$ , some peaks are identified from their position in the spectra at the two angles as due to the  $(d, ^3\text{He})$  reaction on  $^{12}\text{C}$ ,  $^{13}\text{C}$ ,  $^{14}\text{N}$ ,  $^{16}\text{O}$ ,  $^{24}\text{Mg}$ , and  $^{26}\text{Mg}$  nuclei. These peaks are presented in Fig. 1 labeled with the excitation energies in the final nuclei.

The same method of analysis used in Refs. [3] and [4] was employed to extract the focal plane positions and integrated counts of the individual peaks in the experimental spectra. They were analyzed with the same multipeak-fitting computer code and, in this work also, special attention was paid to verifying that the final results obtained from the computer analysis were not dependent upon the initial conditions (values of peak positions and shapes of reference peaks) which were used.

Absolute cross sections for the reaction at each angle were obtained from the integrated counts in each peak by taking into account the integrated charge and by using the known values of the number of  $^{25}\text{Mg}$  nuclei in the target and the spectrograph solid angle. The accuracy assigned to these cross sections is obtained by combining the uncertainties in the number of  $^{25}\text{Mg}$  nuclei ( $\sim 5\%$ ), the solid angle ( $\sim 4\%$ ), and the integrated charge ( $\sim 1\%$ ) with the one arising from the counting statistics.

### III. EXCITATION ENERGIES

The two spectra measured with the  $^{25}\text{Mg}$  target were obtained in the same run and with the same tuning of the detection system as the ones measured in the previous studies on the  $^{27}\text{Al}$  and  $^{29}\text{Si}$  targets, so that the same procedure could be used in this work to determine the excitation energies from the peak positions of the two spectra. This procedure is based on a relationship between the radius of curvature of the  $^3\text{He}$  particle's trajectory in the spectrograph and the corresponding peak position in the counter.

This relationship was calibrated with 12 peaks which are strongly populated at  $\theta_{\text{lab}}=10^\circ$  in the  $^{31}\text{P}(d,^3\text{He})^{30}\text{Si}$  reaction. They correspond to levels of  $^{30}\text{Si}$  whose excitation energies are known [2] with an accuracy ranging from a few hundreds of eV to, in the worst case, 2 keV. The  $^{31}\text{P}(d,^3\text{He})^{30}\text{Si}$  reaction was studied concurrently with the present experiment, in the same experimental conditions, and spectra were measured at  $\theta_{\text{lab}}=10^\circ$  and at five different values of the spectrograph magnetic field in order to calibrate the entire length of the counter. With this calibration, excitation energies can be obtained with an accuracy of  $\pm 5$  keV.

Since the spectra were measured at two angles only, the following criteria were adopted in order to safely make the assignment of an experimental peak to the population of a level in one of the various final nuclei.

(i) Peaks which are observed at the two angles will be considered as due to the population of the same level whenever the excitation energy values obtained at each angle are in agreement within 5 keV. The adopted value of the excitation energy is then the mean value of the two determinations.

(ii) A level observed in this work will be identified with a level of the current literature only if the excitation energy values are in a mutual agreement within error limits.

(iii) A peak which is observed at only one angle will be considered as corresponding to a  $^{24}\text{Na}$  level only if it cannot correspond to any of the levels which are known to be populated in the  $(d,^3\text{He})$  reaction on one of the six nuclei noted in Sec. II as being present in the target.

(iv) A level from this work which has no correspondent in the current literature will be presented as a new level *only* if the experimental peak is observed at the two angles (it is worth pointing out that the application of this criterion led to the rejection of five peaks only).

With these procedures, 56 peaks are attributed to the population of  $^{24}\text{Na}$  levels. Seven of them could be observed at only one angle (five at  $\theta_{\text{lab}}=10^\circ$  and two at  $\theta_{\text{lab}}=18^\circ$ ) because they are obscured at the other angle by peaks due to the  $(d,^3\text{He})$  reaction on the carbon and oxygen nuclei. These excitation energy values are presented in Table I (column 3) and compared there with the set of values from Ref. [2] (column 1). This comparison leads to the identification of 47 of these 56 peaks with levels of Ref. [2], the excitation energies of which are adopted in the remainder of this paper whenever the error in Ref. [2] is less than 5 keV.

Sixteen of the eighteen peaks observed in the previous study at  $E_d=52$  MeV [6] can be identified with levels or groups of levels observed in this work. These levels also are listed in Table I (column 4). These identifications are based upon the similitude of the excitation energies and upon the comparison of the relative sizes of the peaks in Fig. 4 of Ref.

[6] and in Fig. 1 of this work.

The first nine peaks observed in Ref. [6] below 3.6 MeV, all of which can be identified with levels, or groups of levels, known in the literature (Ref. [1]) can be analyzed as follows. Four peaks, at  $E_x=0.532\pm 0.014$ ,  $1.884\pm 0.013$ ,  $2.538\pm 0.012$ , and  $2.911\pm 0.012$  MeV, correspond actually to the population of two levels each. These are resolved in the present work:  $E_x=0.472$  and  $0.563$  MeV,  $1.846$  and  $1.886$  MeV,  $2.514$  and  $2.563$  MeV, and  $2.904$  and  $2.978$  MeV, respectively (Table I and Fig. 1). A fifth peak, at  $E_x=1.352\pm 0.013$  MeV, can correspond to the population of the triplet of levels at  $E_x=1.341$ ,  $1.345$ , and  $1.347$  MeV, which cannot be resolved in this work. This point will be considered later in Sec. V. The remaining four other peaks are due to the population of single levels; the one at  $E_x=3.369\pm 0.014$  MeV (which has been identified in Ref. [1] with the level at  $E_x=3.372$  MeV,  $J^\pi=2^-$ ) is the first state to be populated through a  $l_p=1$  transition.

Of the nine peaks of Ref. [6] with  $E_x>3.6$  MeV which were not identified in Ref. [1], those at  $E_x=3.928\pm 0.014$ ,  $4.520\pm 0.012$ ,  $5.239\pm 0.016$ ,  $6.904\pm 0.029$ , and  $7.067\pm 0.013$  MeV are also populated through  $l_p=1$  transitions. The  $E_x=4.520\pm 0.012$  MeV peak of Ref. [6] corresponds to the peak observed in this work at  $E_x=4.524$  MeV (Fig. 1). It could result from the simultaneous population of the two known levels [2] at  $E_x=4.526\pm 0.006$  and  $4.562$  MeV. By using the multipeak-fitting computer code, it is found that the lower level accounts for more than 95% of the total area of the peak. The higher level, at  $E_x=4.562$  MeV, is not indicated in the Fig. 1 nor in the column 3 of Table I because its observation does not seem definitely established from the present data. The four other of these  $l_p=1$  peaks of Ref. [6] correspond to the apparently single peaks which are observed in this work at  $E_x=3.934$ ,  $5.243$ ,  $6.905$ , and  $7.084$  MeV, respectively (Fig. 1 and Table I).

The two peaks observed in Ref. [6] at  $E_x=3.652\pm 0.019$  and  $4.939\pm 0.013$  MeV are populated through  $l_p=2$  transitions (see Table I). As it can be seen in Fig. 1 and Table I, the first peak corresponds to the population of the two levels observed in the present work at  $E_x=3.628$  and  $3.656$  MeV,  $J^\pi=3^+$  and  $2^+(1^+)$ , respectively, and which are populated with very similar intensities, and the second peak to the population of the four levels at  $E_x=4.891$ ,  $4.907$ ,  $4.939$ , and  $4.973$  MeV. The contribution of each of these four levels to the summed intensity was estimated to be about 20, 35, 10, and 35 %, respectively, by using the multipeak-fitting computer code. The  $J^\pi$  values are known only for the levels at  $E_x=4.891$  MeV ( $J^\pi=(3^+, 4^-, 5^+)$ , Ref. [2]) and  $4.939$  MeV ( $J^\pi=(1-3)^-$ , Ref. [9]). The two levels at  $E_x=4.907$  and  $4.973$  MeV, which are the ones most strongly populated in this work, are probably positive-parity states, since the total peak in Ref. [6] is populated through a  $l_p=2$  transition. The excitation energy of this peak quoted in Ref. [6] is in a good agreement with the mean value of the excitation energies of the two levels at  $E_x=4.907$  and  $4.973$  MeV.

Two weakly populated peaks were observed in Ref. [6] at  $E_x=7.188\pm 0.029$  and  $7.552\pm 0.029$  MeV. On the basis of these excitation energies, the first peak could correspond to the population of one or several of the levels of Ref. [2] at  $E_x=7.163$ ,  $7.186$ ,  $7.187$ , and  $7.192$  MeV (Table I). However, no peak was observed in the present study which could cor-

TABLE I.  $^{25}\text{Mg}(d, ^3\text{He})^{24}\text{Na}$ : spectroscopic information from this work and from other sources.

$E_x^c$ (MeV $\pm$ keV)	Ref. [2] $J^\pi$	This work <sup>a</sup> $E_x$ (MeV)	Ref. [6] <sup>b</sup> $E_x$ (MeV)	Ref. [2] $E_x^c$ (MeV $\pm$ keV)	$J^\pi$	This work <sup>a</sup> $E_x$ (MeV)	Ref. [6] <sup>b</sup> $E_x$ (MeV)
0	$4^+$	0	0	5.192	$3^-$	5.189	
0.472	$1^+$	0.475	} $0.532 \pm 0.014$	5.250 $\pm$ 2	$3^-$	5.243	} $5.239 \pm 0.016$
0.563	$2^+$	0.568		5.339	$2^-$	5.335	
1.341	$2^+$	} 1.348	} $1.352 \pm 0.013$	5.397	} $(1-3)^-$	} 5.402 <sup>d</sup>	
1.345	$3^{(+)}$			5.432 $\pm$ 8			
1.347	$1^+$					5.476 <sup>e</sup>	
1.512	$5^+(3^+)$			1.514	$1.495 \pm 0.013$	5.479	
1.846	$2^+$	1.845	} $1.884 \pm 0.013$	5.585 $\pm$ 8	} $\pi=U$	} 5.627	
1.886	$3^+$	1.883		5.628			
2.514	$3^+$	2.511	} $2.538 \pm 0.012$	5.660 $\pm$ 20	} 5.720 $\pm$ 20	} 5.733	
2.563	$4^+(2^+)$	2.560		5.774 $\pm$ 5			
2.904	$3^+$	2.905	} $2.911 \pm 0.012$	5.810	} 5.846	} 5.863	
2.978	$2^+(3^+)$	2.978					
3.217	$4^+(2^+)$	3.214	$3.237 \pm 0.015$				
3.372	$2^-$	3.371	$3.369 \pm 0.014$	5.863			
3.413	$1^+$	3.413		5.918			
3.589	$1^+$			5.953			
3.628	$3^+$	3.630	} $3.652 \pm 0.019$	5.966	} $0^+ f$	} 6.223	
3.656	$2^+(1^+)$	3.657		6.073			
3.682	$0^+$			6.222			
3.745	$3^-$	3.745		6.248			
		3.884		6.578 $\pm$ 4			
3.896 $\pm$ 6	$(1-3)^-$					6.715	
3.936	$(0^+ - 4^+)$	3.934	$3.928 \pm 0.014$			6.787	
3.943	$(2^+ - 6^+)$					6.846	
3.977	$(1^-, 2^+)$	3.974 <sup>d</sup>				6.905	$6.904 \pm 0.029$
4.048	$0^-$			6.962	$1^+$		
4.145	$4^-(5^-)$	4.140 <sup>e</sup>		6.967			
4.187	$2^+$	} 4.194 <sup>e</sup>		6.993	} $3^-$		
4.196	$(1, 2)^-$					7.010	
4.207	$2^+$			7.069			
4.220 $\pm$ 3				7.072			
4.442	$2^-$	4.438				7.084	$7.067 \pm 0.013$
4.459 $\pm$ 8				7.086	$0^-$		
4.526 $\pm$ 8	$3^-$	4.524	$4.520 \pm 0.012$	7.097			
4.562	$1^-$			7.142		7.144 <sup>e</sup>	
4.622		4.619		7.151	$1^-$		
4.692		4.692		7.163	$0^-$		
4.751	$2^-$	4.751		7.186	} $2^-$	} $7.188 \pm 0.029$	
4.772 $\pm$ 7				7.187			
4.891	$(3^-, 4^+, 5^-)$	4.888		7.192			
		4.907		7.246			
4.939	$(1, 3)^-$	4.936	$4.939 \pm 0.013$	7.246	$2^+$	} 7.246 <sup>g</sup>	
4.980 $\pm$ 7		4.973		7.252	$1^-$		
5.030 $\pm$ 2		5.028				7.313	
5.045	$(1-3)^-$			7.324			
5.060	$2^-$	5.055		7.328	$1^-$		
5.117	$1^-$	5.115					
5.160 $\pm$ 8							

<sup>a</sup>The excitation energies are given with an accuracy of  $\pm 5$  keV.

<sup>b</sup>From the study of the  $^{25}\text{Mg}(d, ^3\text{He})^{24}\text{Na}$  reaction at  $E_d=52$  MeV.

<sup>c</sup>If  $\Delta E_x$  is less than 1 keV in Ref. [2], the excitation energy is rounded off to the next keV.

<sup>d</sup>The corresponding peak was observed at  $\theta_{\text{lab}}=18^\circ$  only.

<sup>e</sup>The corresponding peak was observed at  $\theta_{\text{lab}}=10^\circ$  only.

<sup>f</sup>This level is the first  $T=2$  state in  $^{24}\text{Na}$ . Therefore, its population through the  $(d, ^3\text{He})$  reaction is isospin forbidden.

<sup>g</sup>Due to the relative population at the two angles, the experimental peak at  $E_x=7.246$  MeV seems to correspond to the negative-parity state (see Sec. IV).

respond to the peak at  $E_x=7.188 \pm 0.029$  MeV (Fig. 1). The peak at  $E_x=7.552 \pm 0.029$  MeV is out of the range of excitation energy considered in this work.

Finally, it can be seen in Table I that ten levels observed in the present work do not have correspondents among the

levels of Ref. [2]. The level at  $E_x=3.884$  MeV is not identified with the level at  $E_x=3.896 \pm 0.006$  MeV of Ref. [2] because the second of the above quoted criteria (consistency of the excitation energy values) is not fulfilled. Therefore, it is presented in Table I as a new level along with the six

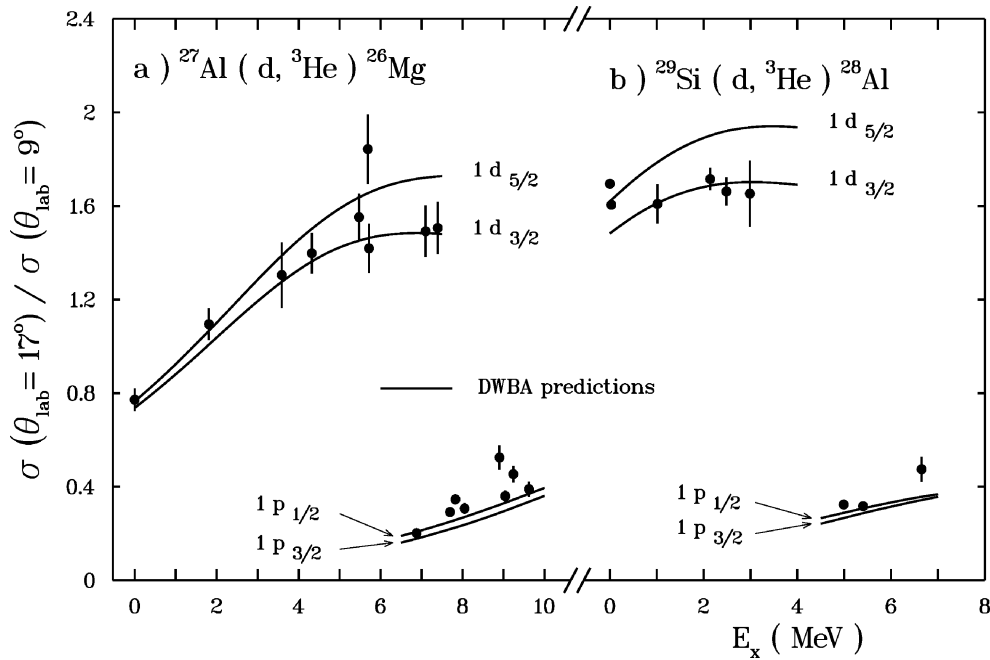


FIG. 2. Ratios of the cross sections at  $\theta_{\text{lab}}=9^\circ$  and  $17^\circ$  for the  $(d, {}^3\text{He})$  reaction at  $E_d=29$  MeV on  ${}^{27}\text{Al}$  and  ${}^{29}\text{Si}$  nuclei. The points are the experimental values. Only the counting statistics is taken into account in the error bars. Curves result from DWBA calculations done for  $1d_{5/2}$ ,  $1d_{3/2}$  and  $1p_{1/2}$  transitions. (a)  ${}^{27}\text{Al}(d, {}^3\text{He}){}^{26}\text{Mg}$  reaction. The levels populated through  $l_p=2$  transitions are the levels at  $E_x=0$ , 1.809, 3.589, 4.318, 5.474, 5.690, 5.716, 7.100, and 7.395 MeV. The levels populated through  $l_p=1$  transitions are the levels at  $E_x=6.878$ , 7.694, 7.824, 8.050, 8.902, 9.042, 9.239, and 9.618 MeV (see Ref. [3]). (b)  ${}^{29}\text{Si}(d, {}^3\text{He}){}^{28}\text{Al}$  reaction. The levels populated through  $l_p=2$  transitions are the levels at  $E_x=0$ , 0.031, 1.014, 2.139, 2.486, and 2.988 MeV. The levels populated through  $l_p=1$  transitions are the levels at  $E_x=4.998$ , 5.406, and 6.652 MeV (see Ref. [4]).

levels at  $E_x=4.907$ , 5.452, 5.846, 6.715, 6.787, 6.846, and 7.313 MeV. The remaining two levels, at  $E_x=6.905$  and 7.084 MeV, have been identified above with peaks observed in Ref. [6]. The level at  $E_x=7.084$  MeV is not identified with the level at  $E_x=7.086$  MeV which is assigned  $J^\pi=0^-$  in Ref. [2] because such a level could be populated in a single step direct transfer only through the unlikely pickup of the proton in the  $1f_{5/2}$  orbit.

#### IV. IDENTIFICATION OF THE $l_p=1$ STATES

In the study of the  $(d, {}^3\text{He})$  reaction done at  $E_d=29$  MeV on  ${}^{27}\text{Al}$  [3] and  ${}^{29}\text{Si}$  [4], the orbital angular momenta of the transferred proton and the spectroscopic factors were obtained by comparing the experimentally measured angular distributions with the DWBA calculations done with the code DWUCK4 [10]. It was observed that the experimental angular distributions corresponding to the  $l_p=1$  and  $l_p=2$  transitions are accounted for quite well by the DWBA calculations even though this agreement becomes poorer with increasing excitation energy for the  $l_p=2$  transitions. A striking feature of these calculations is that the angular behavior of the  $l_p=1$  and 2 transitions is different enough to make the distinction between them clear without measuring the complete angular distributions simply by comparing with the DWBA cross sections at a couple of forward angles.

This is demonstrated in the Figs. 2(a) and 2(b) for the  ${}^{27}\text{Al}$  and  ${}^{29}\text{Si}$  target nuclei, respectively. In these figures, the ratios of the experimental cross sections obtained at  $\theta_{\text{lab}}=9^\circ$  and  $17^\circ$  during the angular distribution measurements for some levels populated through  $l_p=1$  and  $l_p=2$  transitions

are presented along with the ratios of the DWBA cross sections calculated at these two angles. The experimental errors are from counting statistics only. For these two nuclei, the measured as well as calculated cross sections are markedly smaller at  $\theta_{\text{lab}}=17^\circ$  than at  $\theta_{\text{lab}}=9^\circ$  for the  $l_p=1$  transitions, whereas they are larger for those with  $l_p=2$  (with the exception of the  $l_p=2$  transition to the ground state of  ${}^{26}\text{Mg}$ ). Thus it was concluded that the comparison of the spectra measured at these two angles leads to an unambiguous distinction between the  $l_p=1$  and  $l_p=2$  transitions.

Such a comparison is made also in the present study of the  ${}^{25}\text{Mg}(d, {}^3\text{He}){}^{24}\text{Na}$  reaction in order to distinguish the  $l_p=1$  transitions. The DWBA cross sections were obtained at  $\theta_{\text{lab}}=10^\circ$  and  $18^\circ$  from local and zero-range DWUCK4 calculations for  $l_p=1$  and  $l_p=2$  transitions using the optical parameters of Table II. As in the previous Orsay work [3,4], the deuteron optical parameters are adapted for the  ${}^{25}\text{Mg}$  target nucleus from the relationships ( $L$  potential) presented in Ref. [11]. The  ${}^3\text{He}$  optical parameters are from the analysis of 25 MeV  ${}^3\text{He}$  elastic scattering [7] from  ${}^{23}\text{Na}$ .

It has been checked that the  $9^\circ$  to  $17^\circ$  DWBA ratios do not differ significantly from the  $10^\circ$  to  $18^\circ$  DWBA ratios. As was the case for most of the  $l_p=2$  transitions calculated for the  ${}^{26}\text{Mg}$  and  ${}^{28}\text{Al}$  final nuclei, the DWBA cross sections for the  $l_p=2$  transitions to the  ${}^{24}\text{Na}$  final nucleus are smaller at the more forward angle so that the ratio of the  $10^\circ$ – $18^\circ$  DWBA cross sections is larger than 1. On the other hand, the ratio of the  $10^\circ$ – $18^\circ$  DWBA cross sections calculated for the  $1p$  transitions varies continuously from 0.12 to 0.44 for excitation energies from 3.0 to 7.5 MeV (Fig. 3). As a consequence, the following criterion was adopted: only  ${}^{24}\text{Na}$  lev-

TABLE II. Optical model parameters used in DWBA calculations.

Channel	$V$ (MeV)	$r_r$ (fm)	$a_r$ (fm)	$W_V$ (MeV)	$4W_D$ (MeV)	$r_i$ (fm)	$a_i$ (fm)	$V_{s.o.}$ (MeV)	$r_{s.o.}$ (fm)	$a_{s.o.}$ (fm)	$r_c$ (fm)
$^{25}\text{Mg} + d$	84.6	1.17	0.758	1.1	47.6	1.325	0.735	6.49	1.07	0.66	1.30
$^{23}\text{Na} + ^3\text{He}$	227.6	1.15	0.637	23.9		1.537	0.890				1.40
Proton	<sup>a</sup>	1.25	0.65					$\lambda=25$	1.25	0.65	1.25

<sup>a</sup>The depth is adjusted by the code DWUCK4.

els for which the ratio of the experimental cross sections is in agreement to within a factor of 2 with the DWBA predicted ratio for the  $1p$  transitions have been considered in this work as candidates for  $l_p=1$  proton pickup. This criterion is fulfilled by the twelve levels which are presented in Table III and Fig. 3. They can be assigned  $J^\pi=(1-4)^-$ .

The validity of this method of identifying the  $l_p=1$  transitions is supported by the fact that ten of these twelve levels were identified in Sec. III and in Table I with the six levels populated through  $l_p=1$  proton pickup in Ref. [6] and/or with levels which have been assigned negative parity in Ref. [2], based on Refs. [12–17]. References [12–14] report on results of  $\gamma$ -decay experiments, Ref. [15] on the  $^{23}\text{Na}(d,p)^{24}\text{Na}$  reaction, Ref. [16] on the  $^{22}\text{Ne}(^3\text{He},p)^{24}\text{Na}$  reaction, and Ref. [17] on the  $^{26}\text{Mg}(\vec{d},\alpha)^{24}\text{Na}$  reaction at  $\theta=180^\circ$ . These levels, from Refs. [2] and [6], are presented in Table III, columns 6 and 8, respectively. The  $J^\pi$  values which result from the combination of the previous  $J^\pi$  assignments with the present ones are presented for these twelve levels in Table III, column 5.

A further check of the validity of this method is provided by the observation in the current measurements of the two  $^{23}\text{Na}$  levels at  $E_x=2.640$  and  $3.678$  MeV,  $J^\pi=1/2^-$  and  $3/2^-$ , respectively (see Fig. 1). They result from the  $(d, ^3\text{He})$  reaction on the small ( $\sim 4\%$ ) amount of  $^{24}\text{Mg}$  present in the

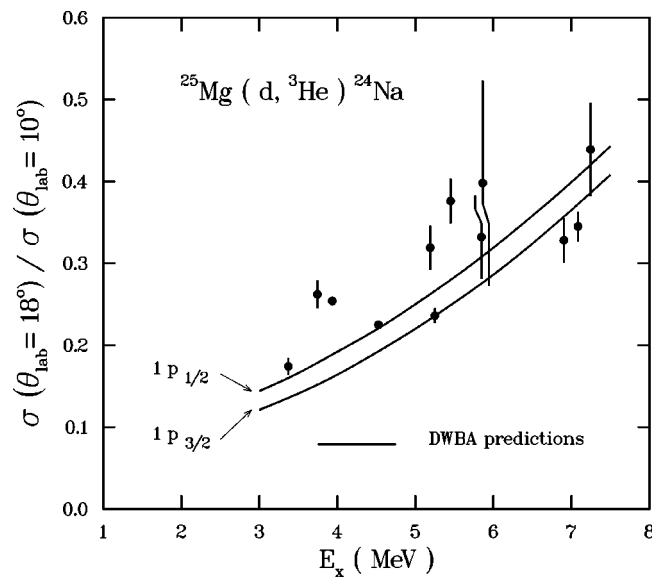


FIG. 3. Ratios of the cross sections at  $\theta_{\text{lab}}=10^\circ$  and  $18^\circ$  for the  $^{25}\text{Mg}(d, ^3\text{He})^{24}\text{Na}$  reaction at  $E_d=29$  MeV. The points are the experimental values. Only the counting statistics are taken into account in the error bars. Curves result from DWBA calculations done for  $1p_{1/2}$  and  $1p_{3/2}$  transitions.

$^{25}\text{Mg}$  target. The ratios of the experimental as well as DWBA cross sections for these two levels are also presented in Table III and they are consistent with the populations through  $1p_{1/2}$  and  $1p_{3/2}$  transitions, respectively, which were established in Ref. [6].

The  $J^\pi$  value of the level at  $E_x=3.936$  MeV is listed in Ref. [2] as  $(0^+-4^+)$ . This level is assigned  $(1-3)^-$  in Table III on the basis of the present work, consistent with Ref. [6]. This assignment could be restricted, still further, to  $(2,3)^-$  if the population of this level through a  $1p_{1/2}$  transfer is assumed. This assumption is reasonable since the lowest strongly populated negative-parity state observed in the  $(\vec{d}, ^3\text{He})$  reaction at  $E_d=52$  MeV on the  $^{16,18}\text{O}$ ,  $^{20,22}\text{Ne}$ ,  $^{24,26}\text{Mg}$ , and  $^{28}\text{Si}$  even-even nuclei is due to the pickup of  $1p_{1/2}$  protons [18].

The assumption of the population of the level at  $E_x=4.524$  MeV through a  $1p_{1/2}$  transition also seems probable for the following reasons:

(i) due to the  $J^\pi=5/2^+$  value of the ground state of  $^{25}\text{Mg}$ , the  $1p_{1/2}$  strength is expected to be shared between at least two levels with  $J^\pi=2^-$  and  $3^-$ , respectively.

(ii) the difference between the excitation energies of the two levels at  $E_x=3.936$  and  $4.524$  MeV is only about 600 keV, whereas in the neighboring nuclei  $^{23}\text{Na}$  and  $^{25}\text{Na}$  the first two levels carrying a substantial portion of the  $1p_{1/2}$  and  $1p_{3/2}$  strengths are separated by more than 1 MeV. Such a situation was already pointed out in the case of the  $^{29}\text{Si}(d, ^3\text{He})^{28}\text{Al}$  reaction [4].

By using these considerations, the most likely  $J^\pi$  value of the level at  $E_x=3.936$  MeV would be  $2^-$  since the level at  $E_x=4.524$  MeV is assigned  $J^\pi=3^-$  in [2].

If one assumes that the experimental angular distributions of the levels populated through  $l_p=1$  transitions in  $^{24}\text{Na}$  are accounted for by the DWUCK4 calculations as well as they are in  $^{26}\text{Mg}$  and  $^{28}\text{Al}$ , values of  $C^2S$  can be extracted at each of the two angles for each of the levels presented in Table III by using a relationship which connects the experimental and DWBA cross sections

$$\left(\frac{d\sigma(\theta)}{d\omega}\right)_{\text{c.m.}} = 2.95 \frac{C^2 S_{l=1,j}}{(2j+1)} \left(\frac{d\sigma_{l=1,j}(\theta)}{d\omega}\right)_{\text{DWUCK4}} \quad (1)$$

In this relationship, 2.95 is the commonly adopted value for the normalization factor of the  $(d, ^3\text{He})$  reaction [19],  $j$  is the total angular momentum of the transferred proton ( $1/2$  or  $3/2$  in the present case), and  $S_{l=1,j}$  is the spectroscopic factor. The isospin coupling Clebsch-Gordan coefficient  $C^2$  is equal to  $2/3$  for this reaction.

As can be seen in Fig. 4, this assumption is not inconsistent with the experimental cross sections available for the

TABLE III. States populated through  $l_p=1$  transitions in the ( $d, {}^3\text{He}$ ) reaction.

$E_x$ (MeV)	This work		$C^2S$	$J^\pi$ <sup>b</sup>	Ref. [2]		Ref. [6]		$C^2S$
	Ratio <sup>a</sup> Exp.	DWBA			$E_x$ (MeV)	$J^\pi$	$E_x$ (MeV)	$nlj$	
(a) ${}^{24}\text{Na}$									
3.371	$0.17 \pm 0.02$	0.15	0.08	$2^-$	3.372	$2^-$	$3.369 \pm 0.014$	$1p_{3/2}$	0.15
3.745	$0.26 \pm 0.02$	0.17	0.06	$3^-$	3.745	$3^-$			
3.934	$0.25 \pm 0.02$	0.18	0.70	$(1-3)^-{}^c$	3.936	$(0^+-4^+)$	$3.928 \pm 0.014$	$1p_{1/2}$	1.18
4.524	$0.23 \pm 0.02$	0.21	0.59	$3^-$	$4.526 \pm 0.008$	$3^-$	$4.520 \pm 0.012$	$1p_{3/2}$	0.78
5.189	$0.27 \pm 0.04$	0.25	0.05	$3^-$	5.192	$3^-$			
5.243	$0.24 \pm 0.02$	0.26	0.21	$3^-$	$5.250 \pm 0.002$	$3^-$	$5.239 \pm 0.016$	$1p_{3/2}$	0.40
5.452	$0.38 \pm 0.04$	0.26	0.08	$(1-4)^-$					
5.846	$0.33 \pm 0.06$	0.30	0.02	$(1-4)^-$					
5.863	$0.40 \pm 0.13$	0.30	0.008	$(1-4)^-$	5.863				
6.905	$0.33 \pm 0.03$	0.38	0.09	$(1-4)^-$			$6.904 \pm 0.029$	$1p_{3/2}$	0.29
7.084	$0.35 \pm 0.03$	0.40	0.22	$(1-4)^-$			$7.067 \pm 0.013$	$1p_{3/2}$	0.52
7.246	$0.44 \pm 0.06$	0.37	$0.04^d$	$1^-$	7.246	$1^-$			
(b) ${}^{23}\text{Na}$									
2.640	$0.15 \pm 0.02$	0.11	1.52		2.640	$1/2^-$	$2.644 \pm 0.011$	$1p_{1/2}$	2.64
3.678	$0.19 \pm 0.02$	0.13	0.67		3.678	$3/2^-$	$3.677 \pm 0.010$	$1p_{3/2}$	0.93

<sup>a</sup>This ratio is the value of  $[d\sigma(\theta_{\text{lab}}=18^\circ)/d\omega]_{\text{c.m.}}/[d\sigma(\theta_{\text{lab}}=10^\circ)/d\omega]_{\text{c.m.}}$ .

<sup>b</sup>These  $J^\pi$  values are from the combination of the  $J^\pi=(1-4)^-$  from the pickup of a  $1p$  proton with the  $J^\pi$  values from Ref. [2] (see Sec. IV).

<sup>c</sup>Arguments for assigning this level  $J^\pi=2^-$  are presented in Sec. IV.

<sup>d</sup>Due to the  $J^\pi=1^-$  value of the level at  $E_x=7.246$  MeV in Ref. [2], the  $C^2S$  value was extracted for a  $1p_{3/2}$  transition.

twelve above quoted levels which are candidates for  $l_p=1$  pickup proton. For all these levels, the values of  $C^2S_{l=1}$  determined at each of the two angles differ from the average for the two angles by less than 20%. The average values of  $C^2S$  obtained with the assumption of a  $1p_{1/2}$  transition are presented in Table III (column 4). They would be smaller by about 10% in the case of a  $1p_{3/2}$  transition. These values are substantially smaller than the ones of Ref. [6] presented in the column 9. Such a difference was already pointed out in Refs. [3] and [4] for the  ${}^{26}\text{Mg}$  and  ${}^{28}\text{Al}$  final nuclei, respectively. The summed  $C^2S$  values for the two most strongly populated levels of  ${}^{24}\text{Na}$  at  $E_x=3.936$  and  $4.524$  MeV amount to 1.29. This means that about 65% of the sum-rule limit of 2 for the  $1p_{1/2}$  transitions [20] is exhausted by these two levels. Similar values have been observed in  ${}^{28}\text{Al}$  [4].

## V. COMPARISON BETWEEN EXPERIMENTAL AND SHELL-MODEL SPECTROSCOPIC INFORMATION FOR POSITIVE-PARITY STATES

Many spectroscopic features can be calculated for  ${}^{24}\text{Na}$  levels in the framework of the shell-model in which the USD Hamiltonian [5] is used in a space with active  $2s_{1/2}$ ,  $1d_{3/2}$ , and  $1d_{5/2}$  orbits. In particular, excitation energies and one-proton pickup spectroscopic factors have been calculated in order to compare with the results of the present study of the  ${}^{25}\text{Mg}(d, {}^3\text{He}){}^{24}\text{Na}$  reaction. The total spectroscopic strengths  $\sum C^2S_{nlj}$  calculated for *all* the positive-parity states with  $J^\pi$  values consistent with the single-step direct pickup of a  $sd$  proton from a  $J^\pi=5/2^+$  target nucleus ( $0^+ \leq J^\pi \leq 5^+$ )

amount to 3.099, 0.386, and 0.515 for  $1d_{5/2}$ ,  $2s_{1/2}$ , and  $1d_{3/2}$  transitions, respectively. The results of the calculations are presented in Table IV (columns 1 to 5) for the first eight levels with each of these  $J^\pi$  values. Most of the total spectroscopic strength is concentrated into these first eight levels since the percentage of the strength which is concentrated into these levels amounts to 94, 82, and 88 % for the levels involving  $1d_{5/2}$ ,  $2s_{1/2}$ , and  $1d_{3/2}$  transitions, respectively. In particular, 71% of the total  $1d_{5/2}$  strength is concentrated into the four levels with  $J^\pi=2_1^+$ ,  $3_1^+$ ,  $4_1^+$ , and  $5_1^+$  (with at least 10% of the strength in each individual level).

In the present study, it was assumed that all the levels which have been identified in Table I with positive-parity states of Ref. [2] are populated through *pure*  $l_p=2$  transitions. As it can be seen in Fig. 5, experimental measurements and DWBA predictions compare nicely for fifteen levels with  $E_x < 3.7$  MeV with the exception of the levels at  $E_x=2.904$ ,  $2.978$ , and  $3.413$  MeV. The first two of these are known to be populated through a dominant  $l_p=0$  transition [6] and the third one is very weakly populated ( $< 5 \mu\text{b/sr}$  at the two angles) so that the single-step direct transfer can be not the dominant reaction mechanism. The occurrence of  $l_p=0$  transitions displays the fact that the levels with  $J^\pi=(2,3)^+$  can be populated through the mixture of  $l_p=0$  and  $l_p=2$  transitions. However, it does not seem safe to extract the relative contributions of the two transitions from the present data at the two angles since one does not know the extent to which the experimental shape of a  $l_p=0$  transition is in agreement with the DWBA predictions.

As it was noted previously for the  ${}^{26}\text{Mg}$  and  ${}^{28}\text{Al}$  final

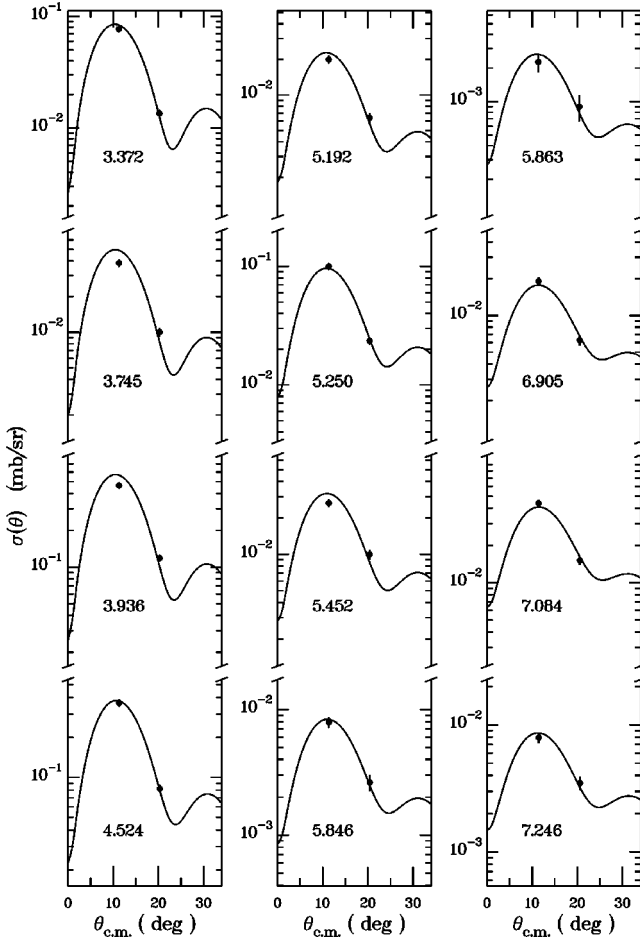


FIG. 4. Experimental cross sections of 12 levels populated through  $l_p = 1$  transitions in the  $^{25}\text{Mg}(d, ^3\text{He})^{24}\text{Na}$  reaction. If not shown, the error is less than the point size. Curves result from the relationship (1) involving the experimental values of  $C^2S$  (Table III, column 4) and the DWBA calculations done with the optical parameters of Table II.

nuclei, the comparison between experiment and DWBA predictions for  $l_p = 2$  transitions becomes poorer at higher excitation energies. So, the positive-parity levels with  $E_x > 3.7$  MeV (most of them being weakly enough populated) are not considered in the following of this discussion.

As in the previous studies of the  $(d, ^3\text{He})$  reaction on  $^{27}\text{Al}$  [3] and  $^{29}\text{Si}$  [4], the identification of the experimental levels with the shell-model ones was done in this work by comparing the corresponding values for excitation energies,  $J^\pi$  values, and spectroscopic factors. This identification is presented in Table V. Experimental values of  $C^2S_{l=2}$  were extracted for the fifteen levels with  $E_x < 3.7$  MeV by comparing the experimental cross sections measured at the two angles with the DWBA-predicted cross sections for *pure*  $l_p = 2$  transitions. The values determined at each of the two angles differ from the average for the two angles by less than 10%, except for the three levels at  $E_x = 2.904$ , 2.978, and 3.413 MeV. The average values which are presented in column 8 of Table V generally agree with the shell-model predictions except for the two weakly populated experimental levels at  $E_x = 1.846$  and 3.413 MeV. Several levels are predicted in Table V to be populated through a substantial mixture of  $l_p = 0$  and  $l_p = 2$  transitions. Since this mixture is not

TABLE IV. Shell-model predictions for excitation energies,  $J^\pi$  values and spectroscopic factors for one nucleon pickup and stripping reactions leading to the  $^{24}\text{Na}$  nucleus.

Excitation energies and $J^\pi$ values		Spectroscopic factors					
$E_x$ (MeV)	$J_i^\pi$	Proton pickup reaction on $^{25}\text{Mg}$			Neutron stripping reaction on $^{23}\text{Na}$		
		$2s_{1/2}$	$1d_{3/2}$	$1d_{5/2}$	$2s_{1/2}$	$1d_{3/2}$	$1d_{5/2}$
0.000	$4_1^+$		0.113	1.505			0.391
0.447	$1_1^+$		0.055	0.166	0.003	0.001	0.688
0.587	$2_1^+$	0.069	0.080	0.544	0.050	0.000	0.289
1.091	$1_2^+$		0.000	0.001	0.351	0.102	0.015
1.132	$2_2^+$	0.011	0.012	0.073	0.283	0.093	0.000
1.373	$3_1^+$	0.064	0.034	0.646		0.025	0.008
1.549	$5_1^+$			0.597			
1.603	$2_3^+$	0.002	0.004	0.002	0.197	0.108	0.089
1.751	$3_2^+$	0.021	0.006	0.106		0.001	0.186
2.179	$3_3^+$	0.008	0.044	0.102		0.104	0.003
2.560	$4_2^+$		0.005	0.240			0.062
2.649	$3_4^+$	0.144	0.155	0.001		0.054	0.026
2.825	$2_4^+$	0.037	0.045	0.002	0.020	0.272	0.009
2.883	$4_3^+$		0.004	0.065			0.004
3.210	$1_3^+$		0.003	0.000	0.299	0.151	0.006
3.329	$0_1^+$		0.000				0.002
3.357	$2_5^+$	0.009	0.017	0.010	0.000	0.120	0.000
3.478	$3_5^+$	0.036	0.025	0.006		0.243	0.001
3.502	$4_4^+$		0.000	0.000			0.032
3.599	$1_4^+$		0.001	0.001	0.000	0.143	0.002
3.778	$3_6^+$	0.016	0.001	0.079		0.000	0.007
3.849	$5_2^+$			0.004			
3.999	$2_6^+$	0.002	0.004	0.004	0.000	0.061	0.003
4.130	$5_3^+$			0.003			
4.263	$4_5^+$		0.004	0.000			0.004
4.481	$2_7^+$	0.042	0.002	0.013	0.141	0.000	0.001
4.489	$1_5^+$		0.002	0.007	0.013	0.023	0.004
4.536	$5_4^+$			0.009			
4.596	$3_7^+$	0.005	0.007	0.058		0.000	0.003
4.665	$5_5^+$			0.022			
4.673	$3_8^+$	0.011	0.010	0.025		0.048	0.002
4.706	$4_6^+$		0.028	0.017			0.000
4.816	$2_8^+$	0.000	0.007	0.002	0.006	0.012	0.038
4.910	$1_6^+$		0.001	0.002	0.014	0.030	0.000
5.084	$1_7^+$		0.000	0.000	0.007	0.018	0.008
5.175	$4_7^+$		0.000	0.053			0.000
5.288	$0_2^+$			0.000		0.001	
5.530	$1_8^+$		0.001	0.000	0.009	0.014	0.000
5.562	$0_3^+$			0.000		0.627	
5.734	$4_8^+$		0.008	0.007			0.000
5.877	$5_6^+$			0.000			
6.181	$0_4^+$			0.000		0.092	
6.189	$5_7^+$			0.000			
6.570	$0_5^+$			0.000		0.073	
6.616	$5_8^+$			0.000			
7.758	$0_6^+$			0.000		0.030	
8.525	$0_7^+$			0.000		0.009	
9.800	$0_8^+$			0.000		0.024	



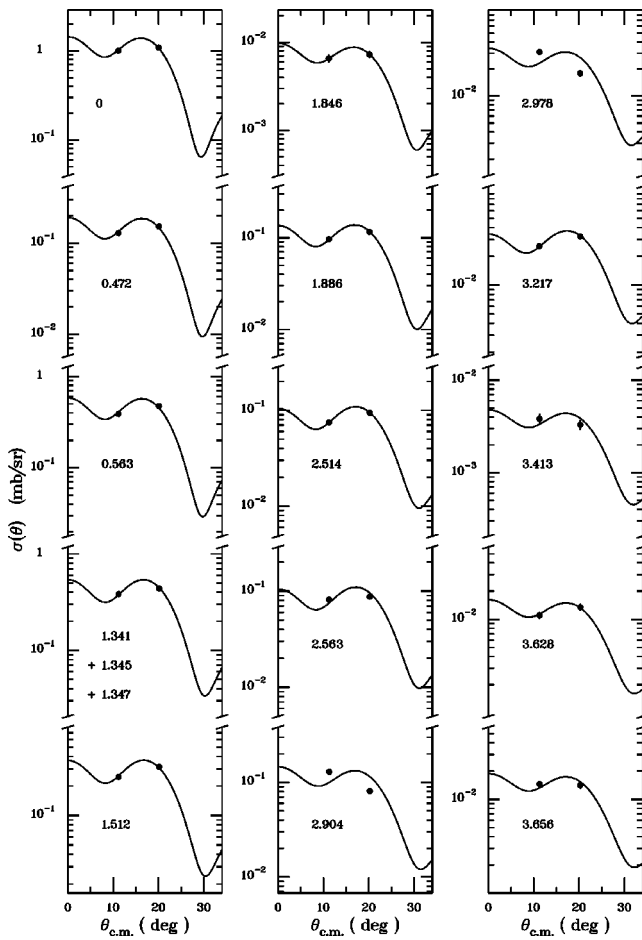


FIG. 5. Experimental cross sections of 15 positive-parity levels populated in the  $^{25}\text{Mg}(d, {}^3\text{He})^{24}\text{Na}$  reaction. If not shown, the error is less than the point size. Curves result from the relationship (1) involving the experimental values of  $C^2S$  (Table V, column 8) and the DWBA calculations done for *pure*  $l_p=2$  transitions with the optical parameters of Table II.

taken into account in the present analysis, only an upper limit of  $C^2S$  is given in Table V for these levels even though the experimental data are correctly accounted for by the DWBA calculations (Fig. 5). Sixteen of the eighteen levels of Ref. [2] which are presented in Table V are involved in the population of nine of the first ten peaks observed in the pickup study at  $E_d=52$  MeV [6] (see Table I). The  $C^2S$  values of Ref. [6] are reported also in Table V (columns 9 and 10). In the case of the  $l_p=2$  transitions, they are in reasonable agreement with the shell-model predictions, with the exception of the peak at  $E_x=2.911\pm 0.012$  MeV for which no  $l_p=2$  strength was observed. On the other hand, in the case of the  $l_p=0$  transitions, the  $C^2S$ -values quoted in Ref. [6] are substantially larger than those predicted by the shell model.

Other sources of information, such as the results from the study of the  $^{23}\text{Na}(d, p)^{24}\text{Na}$  reaction [15], were also considered in making these identifications. The shell-model predicted spectroscopic factors for the one-neutron stripping reaction on  $^{23}\text{Na}$  ( $J^\pi=3/2^+$ ) are presented also in Table IV (columns 6 to 8) for the first eight levels with  $0^+ \leq J^\pi \leq 4^+$ . The total spectroscopic strengths  $\sum G_{nlj} = (2J_f + 1)(2J_i + 1)^{-1} \sum S_{nlj}$  calculated for *all* the positive-parity states amount to 2.931, 1.557, and 3.512 for the  $1d_{5/2}$ ,  $2s_{1/2}$ , and 1

$d_{3/2}$  transitions, respectively. As for the pickup reaction, most of the total spectroscopic strength (89%) is concentrated upon these first eight levels for both of the  $1d_{5/2}$  and  $2s_{1/2}$  transitions, but 36% of the  $1d_{3/2}$  strength is predicted to lie in shell-model states above the eighth one of each  $J^\pi$ . The experimental  $G_l$  values [15] are presented in the last two columns of Table V. The parentheses are an indication of the difficulty of getting the corresponding  $l_n$  contribution from the DWBA analysis. In any case, these  $G_l$  values are in decent agreement with the shell-model predictions. The observation in Table IV that, in several cases, the same level is predicted to be populated with very different intensities in the stripping and pickup reactions is not unexpected. This difference of population intensity was used as a further tool for identifying the levels at  $E_x=1.846$ , 3.413, 3.589, and 3.628 MeV,  $J^\pi=2^+$ ,  $1^+$ ,  $1^+$ , and  $3^+$ , respectively, which are weakly (or not at all) populated in the pickup reaction with the shell-model levels with  $J^\pi=2_3^+$ ,  $1_3^+$ ,  $1_4^+$ , and  $3_5^+$ , respectively (Table V).

Lastly, a third source of information is to be found in the comparison of the experimental electromagnetic decay rates [2] with the shell-model predictions. Such a comparison was made in Ref. [14] using shell-model calculations done by using the Chung-Wildenthal Hamiltonian [21]. It is presented in Table VI.

By using one or more of these three sources of information, it has been possible to identify the first 19 positive-parity states of  $^{24}\text{Na}$  presented in Ref. [2] with predicted shell-model levels (Table V and Fig. 6). The mean value of the deviation between the experimental and shell-model excitation energies is 161 keV; the largest deviation, 353 keV, is observed for the 3.682–3.329 MeV pair of levels. This pair of levels is identified on the basis of their  $J^\pi$  values and of the agreement between the experimental and shell-model predicted electromagnetic decay rates (Table VI). The  $J^\pi=0_1^+$  level is predicted to exhibit very little single-particle character, and actually the  $J^\pi=0^+$  level at  $E_x=3.682$  MeV is observed neither in the pickup nor in the stripping reactions. These values of the mean and largest deviations are quite similar to the ones obtained in the  $^{26}\text{Mg}$  and  $^{28}\text{Al}$  nuclei (Table VII).

The levels at  $E_x=1.345$ , 1.512, 2.563, 2.978, 3.217, and 3.656 MeV, for which the removal of the ambiguities in the  $J^\pi$  values in Ref. [2] was one of the goals of the present work, are discussed below.

(a) *The level at  $E_x=1.345$  MeV.* The peak observed in this work at  $E_x=1.348$  MeV can result from the population of at least one of the members of the triplet of levels at  $E_x=1.341$ , 1.345, and 1.347 MeV. On the grounds of the excitation energies,  $J^\pi$  values and  $\gamma$ -decay schemes, the  $J^\pi=2^+$  and  $1^+$  levels at  $E_x=1.341$  and 1.347 MeV, respectively, can be safely identified with the shell-model predicted levels at  $E_x=1.132$  and 1.091 MeV,  $J^\pi=2_2^+$  and  $1_2^+$ , respectively. These two levels are predicted to be strongly populated in the stripping reaction (Table IV) and the experimentally measured spectroscopic strength of the unresolved peak observed in the  $(d, p)$  reaction [15] is in good agreement with the summed shell-model predictions for these two levels (Table V). On the other hand, these two levels are predicted to be weakly populated in the pickup reaction and it can be

TABLE V. Experimental and shell-model excitation energies,  $J^\pi$  values, and  $C^2S$  values for the one-proton pickup reaction and  $G$  values for the one-neutron stripping reaction leading to the  $^{24}\text{Na}$  nucleus.

Excitation energies and $J^\pi$ values				Proton pickup reaction $C^2S$ values				Neutron stripping reaction						
Ref. [5]		Ref. [2]		Shell model			This work	Ref. [6]		Shell model $G_{n\ell j}$ values <sup>a</sup>			Experimental $G_\ell$ values <sup>b</sup>	
$E_x$ (MeV)	$J^\pi$	$E_x$ (MeV)	$J^\pi$	$2s_{1/2}$	$1d_{3/2}$	$1d_{5/2}$	$l_p=2$	$l_p=0$	$l_p=2$	$2s_{1/2}$	$1d_{3/2}$	$1d_{5/2}$	$l_n=0$	$l_n=2$
0.000	$4_1^+$	0.000	$4^+$		0.075	1.003	0.88		1.37			0.880		0.69
0.447	$1_1^+$	0.472	$1^+$		0.037	0.111	0.13			0.002	0.001	0.516	(0.014)	0.39
0.587	$2_1^+$	0.563	$2^+$	0.046	0.053	0.363	0.42	0.16	0.41	0.063	0.000	0.361	0.10	(0.30)
1.091	$1_2^+$	1.347	$1^+$		0.000	0.001				0.263	0.077	0.011		
1.132	$2_2^+$	1.341	$2^+$	0.007	0.008	0.049	0.48		0.58	0.354	0.116	0.000	0.62	(0.37)
1.373	$3_1^+$	1.345	$3^{(+)}$	0.043	0.023	0.431					0.044	0.014		
1.549	$5_1^+$	1.512	$5^+(3^+)$			0.398	0.34		0.53					
1.603	$2_3^+$	1.846	$2^+$	0.001	0.003	0.001	<0.013 <sup>c</sup>			0.246	0.135	0.111	0.20	(0.39)
1.751	$3_2^+$	1.886	$3^+$	0.014	0.004	0.071	0.14	0.07	0.07		0.002	0.326		0.29
2.179	$3_3^+$	2.514	$3^+$	0.005	0.029	0.068	0.13				0.182	0.005		(0.08)
2.560	$4_2^+$	2.563	$4^+(2^+)$		0.003	0.160	0.14	0.08	0.17			0.140		0.068
2.649	$3_4^+$	2.904	$3^+$	0.096	0.103	0.001	<0.27 <sup>c</sup>				0.095	0.046		
2.825	$2_4^+$	2.978	$2^+(3^+)$	0.025	0.030	0.001	<0.06 <sup>c</sup>			0.025	0.340	0.011		0.42
2.883	$4_3^+$	3.217	$4^+(2^+)$		0.003	0.043	0.054		0.08			0.009		
3.210	$1_3^+$	3.413	$1^+$		0.002	0.000	0.010 <sup>c</sup>			0.224	0.113	0.005	0.22	(0.24)
3.329	$0_1^+$	3.682	$0^+$								0.001			
3.357	$2_5^+$	3.656	$2^+(1^+)$	0.006	0.011	0.007	<0.043 <sup>c</sup>			0.000	0.150	0.000		0.13
3.478	$3_5^+$	3.628	$3^+$	0.024	0.017	0.004	<0.037 <sup>c</sup>		0.11			0.425	0.002	0.27
3.502	$4_4^+$											0.072		
3.599	$1_4^+$	3.589	$1^+$							0.000	0.107	0.002	0.027	(0.09)

<sup>a</sup>In this case ( $^{23}\text{Na}$  target nucleus), the quantity  $G_{n\ell j}$  is equal to  $0.25 \times (2J_i + 1) S_{n\ell j}$  in which  $J_i$  is from the column 2 of this table and  $S_{n\ell j}$  is from Ref. [5].

<sup>b</sup>Reference [15].

<sup>c</sup>The value of  $C^2S$  is obtained with the assumption of a  $1d_{3/2}$  transition which is the dominant shell-model predicted transition.

seen in Table V that their summed shell-model predicted cross sections is very far from accounting for the experimental cross sections measured in this work for the peak at  $E_x=1.348$  MeV. However, if the level at  $E_x=1.345$  MeV,  $J^\pi=3^{(+)}$ , is identified with the shell-model  $J^\pi=3_1^+$  level predicted at  $E_x=1.373$  MeV, the summed experimental cross sections are in good agreement with the summed predicted ones for the three members of the triplet. The  $3_1^+$  member of this triplet would account for about 90% of the pickup population of the peak at  $E_x=1.348$  MeV through a dominant  $l_p=2$  transition. Such a transition was actually observed in Ref. [6]. A further argument in favor of the positive-parity assignment to the level at  $E_x=1.345$  MeV lies in the fact that the  $\gamma$ -decay scheme is in excellent agreement with the shell-model predicted one for the  $J^\pi=3_1^+$  state (Table VI).

(b) *The levels at  $E_x=1.512$  and 2.563 MeV.* The level at  $E_x=1.512$  MeV is assigned  $J^\pi=5^+(3^+)$  in Ref. [2]. There are several arguments in favor of the  $J^\pi=5^+$  assignment. The first one comes from the nice agreement between the experimental and shell-model predicted values for the exci-

tation energy and spectroscopic factor if the level at  $E_x=1.512$  MeV is identified with the  $J^\pi=5_1^+$  shell-model level at  $E_x=1.549$  MeV.

A second argument comes from the consideration of the  $\gamma$ -decay scheme. If the level at  $E_x=1.512$  MeV [ $J^\pi=5^+(3^+)$ ] were not identified with the shell-model level with  $J^\pi=5_1^+$ , it should be identified with the level with  $J^\pi=3_2^+$  because the deviation between the experimental and shell-model excitation energies has been estimated above to be less than (or equal to) 353 keV. The experimental  $\gamma$ -decay scheme of the level at  $E_x=1.512$  MeV (100% towards the ground state, Ref. [2]) is in complete disagreement with the predicted one for the  $J^\pi=3_2^+$  state, which is dominated by an intense transition (95%) towards the  $J^\pi=2^+$  level at  $E_x=0.563$  MeV (Table VI). Therefore, the strong branch (65%) towards the level at  $E_x=0.563$  MeV which is observed in the  $\gamma$  decay of the level at  $E_x=1.886$  MeV ( $J^\pi=3^+$ ) is a further argument for identifying this level with the  $J^\pi=3_2^+$  state, even though the experimentally observed branch towards the ground state (35%) is substantially more

TABLE VI. Electromagnetic decay rates: experimental values<sup>a</sup> and shell-model predictions<sup>b</sup>.

$E_i \rightarrow$ (MeV)	$E_f$ (MeV)= $J_i^\pi \rightarrow J_f^\pi$	0	0.472	0.563	1.341	1.345	1.347	1.512	1.846	1.886
$\downarrow$	$\downarrow$	$4^+$	$1^+$	$2^+$	$2^+$	$3^{(+)}$	$1^+$	$5^+(3^+)$	$2^+$	$3^+$
		$4_1^+$	$1_1^+$	$2_1^+$	$2_2^+$	$3_1^+$	$1_2^+$	$5_1^+$	$2_3^+$	$3_2^+$
0.563	$2^+$	3.8	96.2							
0.587	$2_1^+$	6.2	93.8							
1.341	$2^+$		95.2	4.8						
1.132	$2_2^+$	0.2	98.0	1.8						
1.345	$3^{(+)}$	62		38						
1.373	$3_1^+$	57.2	0.1	42.7						
1.347	$1^+$		100							
1.091	$1_2^+$		68	32						
1.846	$2^+$		25	19	5	11	40			
1.603	$2_3^+$		73.7	10.1	1.8		14.4			
1.886	$3^+$	35		65						
1.751	$3_2^+$	4.3	0.4	94.7	0.4	0.2				
2.514	$3^+$	4		96						
2.179	$3_3^+$	0.1		98.9	0.7	0.3	0.1			
2.563	$4^+(2^+)$	33				52		15		
2.560	$4_2^+$	35.6		2.6		61.3				
2.904	$3^+$	12		3	49	32			4	
2.649	$3_4^+$	58.6	0.1	12.1	13.1	16				
2.978	$2^+(3^+)$	0.6	24	32	33	8				2.1
2.825	$2_4^+$	0.1	20.6	49.4	22.5	5.1	2.2			
3.413	$1^+$		28	11	43		12			5.9
3.210	$1_3^+$		36.7	12.6	43.8		5.6			
3.589	$1^+$		23	69	2.8		3.2		1.7	
3.599	$1_4^+$		45.6	40.4	4.7		8.0			
3.682	$0^+$		100							
3.329	$0_1^+$		93.4	2.4	0.4		3.4			

<sup>a</sup>The experimental excitation energies,  $J^\pi$  values, and electromagnetic decay rates are from Ref. [2]. All the experimental data are typed in roman characters.

<sup>b</sup>The shell-model  $J^\pi$  values and electromagnetic decay rates are from Ref. [14]. They are typed in italic.

intense than the shell-model predicted branch (4%) (Table VI).

Lastly, a third concurring argument comes from a study of the  $(\alpha, d)$  reaction at  $E_\alpha=64$  MeV on the  $^{16}\text{O}$ ,  $^{18}\text{O}$ ,  $^{20}\text{Ne}$ , and  $^{22}\text{Ne}$  target nuclei [22]. Levels strongly populated through  $L=4$  transitions, which have been associated with the transfer of a  $n-p$  pair in a  $(d_{5/2})^2_{J^\pi=5^+}$  state, were observed at  $E_x=1.121$ , 1.824, 1.528, and 1.512 MeV in the  $^{18}\text{F}$ ,  $^{20}\text{F}$ ,  $^{22}\text{Na}$ , and  $^{24}\text{Na}$  nuclei, respectively. Since the first three of these levels are known to be  $J^\pi=5^+$  states [2,23], it can be inferred that the  $J^\pi$  value of the  $^{24}\text{Na}$  level is also  $J^\pi=5^+$ . The nonobservation of this level in the  $^{23}\text{Na}(d, p)^{24}\text{Na}$  reaction [15] can be considered as an indirect argument in favor of the  $J^\pi=5^+$  assignment, since such a level could not be populated in this reaction through the single step direct transfer of a neutron into the  $sd$  shell.

This  $J^\pi=5^+$  assignment is also of importance for the  $J^\pi$  value of the level at  $E_x=2.563$  MeV,  $J^\pi=4^+(2^+)$  [2], since it was pointed out in a study of the electromagnetic decay of some  $^{24}\text{Na}$  states populated in the  $^{23}\text{Na}(d, p\gamma)^{24}\text{Na}$  reaction [24] that the value  $J^\pi=4^+$  would become unique if the level at  $E_x=1.512$  MeV was assigned  $J^\pi=5^+$ . The experimental and shell-model predicted cross sections for the transfer re-

actions (Table V) and  $\gamma$ -decay schemes (Table VI) lead also to the identification of the level at  $E_x=2.563$  MeV with the  $J^\pi=4_2^+$  shell-model level at  $E_x=2.560$  MeV.

(c) *The level at  $E_x=2.978$  MeV.* This level is assigned  $J^\pi=2^+(3^+)$  in Ref. [2]. It could be thus identified with a shell-model level predicted at either  $E_x=2.825$  and 3.478 MeV,  $J^\pi=2_4^+$  and  $3_5^+$ , respectively. The information from the pickup and stripping reactions does not suggest a choice between these two possibilities. The correspondence between the experimental and shell-model excitation energies would favor the  $J^\pi=2^+$  assignment. This assignment is confirmed

TABLE VII. Correspondence of experimental levels with shell-model predicted ones for  $^{24}\text{Na}$ ,  $^{26}\text{Mg}$ , and  $^{28}\text{Al}$ .

Nucleus	Number of identified levels	Mean shift (MeV)	Maximum shift (MeV)	For $J_i^\pi$	Ref.
$^{24}\text{Na}$	19	0.161	0.353	$0_1^+$	a
$^{26}\text{Mg}$	24	0.131	0.293	$4_4^+$	[3]
$^{28}\text{Al}$	21	0.119	0.367	$3_8^+$	[4]

<sup>a</sup>This work.

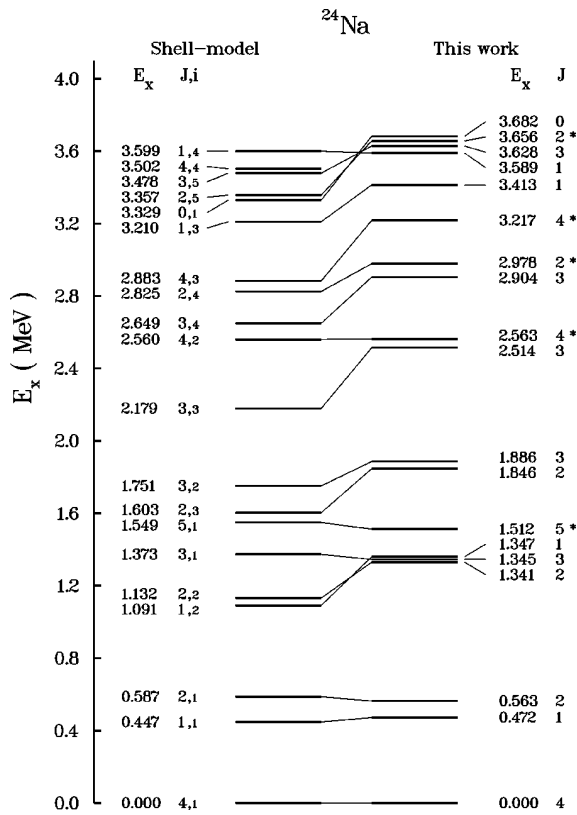


FIG. 6. Identification of experimental positive-parity levels in  $^{24}\text{Na}$  with shell-model predicted levels. This identification is done as explained in the text (Sec. V). The  $i$ th shell-model level with the spin  $J$  is presented in the column  $J, i$ . For the experimental levels, the excitation energies are taken from Ref. [2] and the  $J$  values are from Ref. [2] and from this work. The levels for which ambiguities for the  $J$  values could be removed are indicated with an asterisk.

by the similitude of the  $\gamma$ -decay schemes of the level at  $E_x=2.978$  MeV and of the  $J^\pi=2_4^+$ , shell-model level at  $E_x=2.825$  MeV (Table VI).

(d) *The levels at  $E_x=3.217$  and 3.656 MeV.* These levels are assigned  $J^\pi=4^+(2^+)$  and  $2^+(1^+)$ , respectively, in Ref. [2]. The first one could be identified with one of the shell-

model levels at  $E_x=2.883$  and 3.357 MeV,  $J^\pi=4_3^+$  and  $2_5^+$ , respectively, and the second one with one of the levels at  $E_x=3.357$  and 3.599 MeV,  $J^\pi=2_5^+$  and  $1_4^+$ , respectively. The  $J^\pi=2^+$  assignment is ruled out for the level at  $E_x=3.217$  MeV because in this case a substantial  $l_p=2$  stripping strength, which is not observed experimentally, is predicted by the shell-model calculations. On the other hand, the  $J^\pi=2^+$  assignment is favored for the level at  $E_x=3.656$  MeV because no strength is predicted for the  $J^\pi=1_4^+$  state in the pickup reaction.

## VI. SUMMARY

The present work provides an accurate determination of the excitation energies of many levels populated in the  $^{25}\text{Mg}(d, ^3\text{He})^{24}\text{Na}$  reaction. Most of the peaks from a previous study of this reaction can thus be identified with levels or groups of levels observed in this work. It has been possible to extract valuable spectroscopic information from the present data even though spectra were measured at only two angles. In particular, twelve levels populated through  $l_p=1$  transitions are observed. Furthermore, the first 19 positive-parity experimental levels are identified with shell-model predicted levels by comparing the experimental and shell-model values for various observables such as excitation energies, one-proton pickup spectroscopic factors, one-neutron stripping spectroscopic strengths, and electromagnetic decay rates. These comparisons seem accurate enough to remove the ambiguities existing in the current literature for the  $J^\pi$  values of some states with  $E_x < 3.7$  MeV. They illustrate the efficiency of comprehensive correlations between modern experimental and theoretical results in extending our knowledge of nuclear spectroscopy.

## ACKNOWLEDGMENTS

The authors are indebted to R. Marquette for the  $^{25}\text{Mg}$  target preparation. They acknowledge the operating crew of the Orsay MP Tandem for the efficient running of the accelerator. This work was supported in part by the U.S. National Science Foundation.

- [1] P. M. Endt and C. van der Leun, Nucl. Phys. **A310**, 1 (1978).
- [2] P. M. Endt, Nucl. Phys. **A521**, 1 (1990).
- [3] J. Verotte, G. Berrier-Ronsin, S. Fortier, E. Hourani, J. Kalifa, J. M. Maison, L-H. Rosier, G. Rotbard, and B. H. Wildenthal, Phys. Rev. C **48**, 205 (1993).
- [4] J. Verotte, G. Berrier-Ronsin, S. Fortier, E. Hourani, J. Kalifa, A. Khendriche, J. M. Maison, L-H. Rosier, and G. Rotbard, Phys. Rev. C **49**, 1559 (1994).
- [5] B. H. Wildenthal, Prog. Part. Nucl. Phys. **11**, 5 (1984).
- [6] E. Krämer, G. Mairle, and G. Kaschl, Nucl. Phys. **A165**, 353 (1971).
- [7] J. Verotte, G. Berrier-Ronsin, J. Kalifa, and R. Tamisier, Nucl. Phys. **A390**, 285 (1982).
- [8] J. Verotte, A. Khendriche, G. Berrier-Ronsin, S. Grafeuille, J. Kalifa, G. Rotbard, R. Tamisier, and B. H. Wildenthal, Phys. Rev. C **41**, 1956 (1990).
- [9] P. M. Endt, Nucl. Phys. **A564**, 609 (1993).
- [10] P. D. Kunz (private communication).
- [11] W. W. Daehnick, J. D. Childs, and Z. Vrcelj, Phys. Rev. C **21**, 2253 (1980).
- [12] P. Hungerford, T. von Egidy, H. H. Schmidt, S. A. Kerr, H. G. Börner, and E. Monnard, Z. Phys. A **313**, 325 (1983).
- [13] T. A. A. Tielens, J. Kopecky, K. Abrahams, and P. M. Endt, Nucl. Phys. **A403**, 13 (1983).
- [14] T. A. A. Tielens and J. B. M. De Haas, Nucl. Phys. **A425**, 303 (1984).
- [15] C. Daum, Nucl. Phys. **45**, 273 (1963).
- [16] H. T. Fortune, L. R. Medsker, S. C. Headley, and K. D. Singer, J. Phys. G **4**, 1463 (1978).
- [17] D. O. Boerma, Jahresbericht ETH Zürich, 1975 (unpublished); in Ref. [2].

- [18] G. Mairle, G. J. Wagner, K. T. Knöpfle, Liu Ken Pao, H. Riedesel, V. Bechtold, and L. Friedrich, Nucl. Phys. **A363**, 413 (1981).
- [19] R. H. Bassel, Phys. Rev. **149**, 791 (1966).
- [20] J. B. French and M. H. Macfarlane, Nucl. Phys. **26**, 168 (1961).
- [21] W. Chung, Ph.D. thesis, Michigan State University, 1976.
- [22] Y. Kadota, K. Ogino, K. Obori, Y. Taniguchi, T. Tanabe, M. Yasue, and J. Schmizu, Nucl. Phys. **A458**, 523 (1986).
- [23] F. Ajzenberg-Selove, Nucl. Phys. **A475**, 1 (1987).
- [24] A. S. Keverling Buisman and P. J. M. Smulders, Nucl. Phys. **A228**, 205 (1974).